Binuclear and Tetranuclear Zn(II) Complexes With Thiosemicarbazones: Synthesis, X-ray Crystal Structures, ATP-sensing, DNA-binding, Phosphatase activity and theoretical calculations

Piyali Adak,[a] Bipinbihari Ghosh,[a] Antonio Bauzá,[b] Antonio Frontera,[b] Steven R. Herron,[c] Shyamal Kumar Chattopadhyay[a*]

† Department of Chemistry, Indian Institute of Engineering Science and Technology, Shibpur, Howrah 711 103, India

‡ Department of Chemistry, University of the Balearic Islands, Carretera de Valldemossa km 7.5, 07122 Palma de Mallorca, IllesBalears, Spain

§ Department of Chemistry, Utah Valley University, 800W University Pkwy, Orem UT 84058, USA

Contents

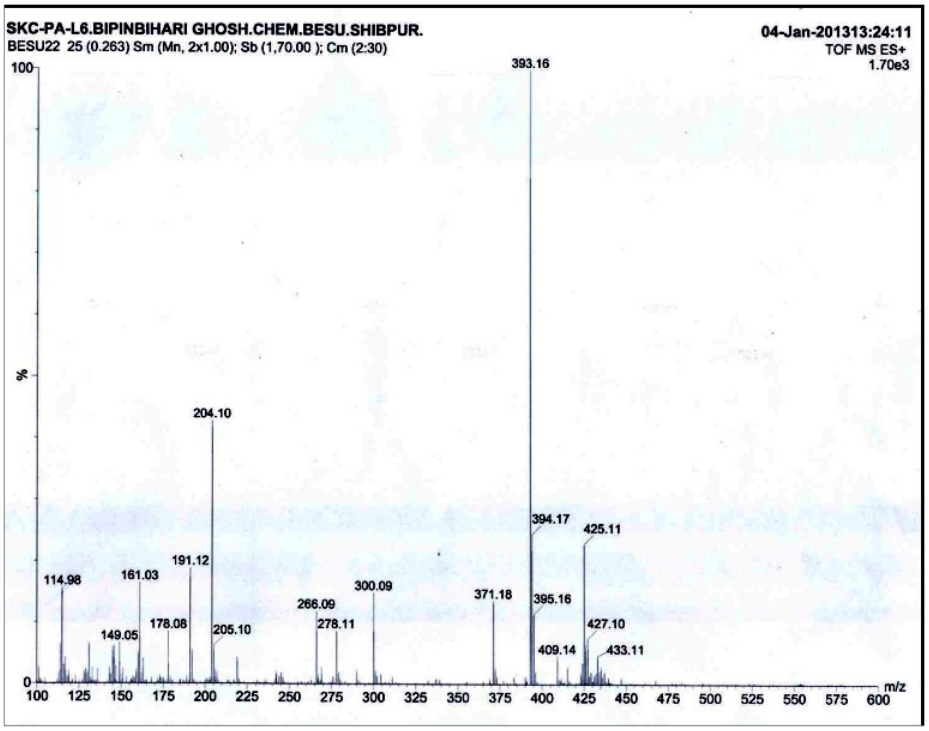

1. Figure S1: Mass spectra of H_2L^1

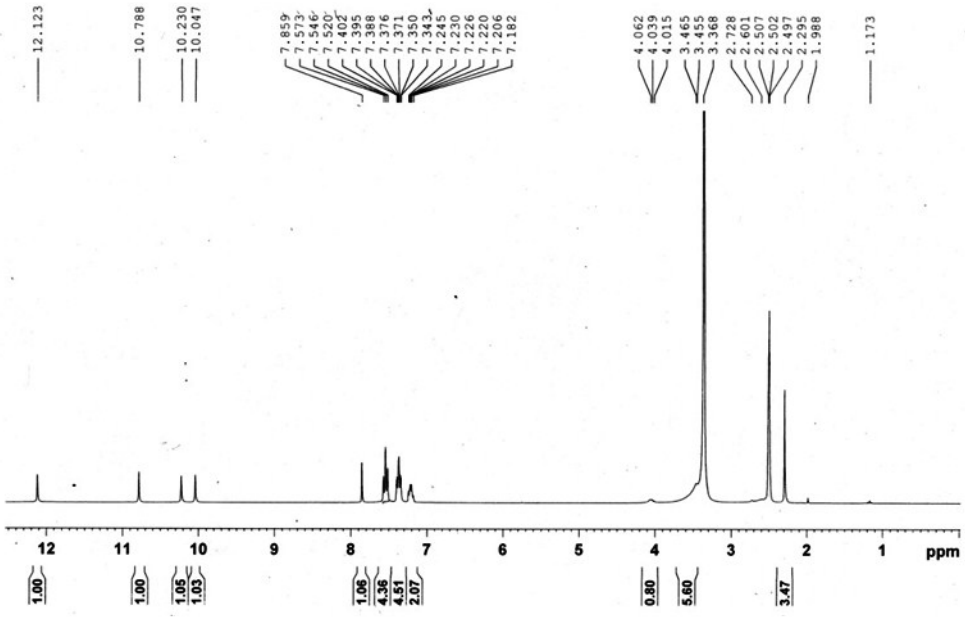

2. Figure S2: NMR spectra of H_2L^1

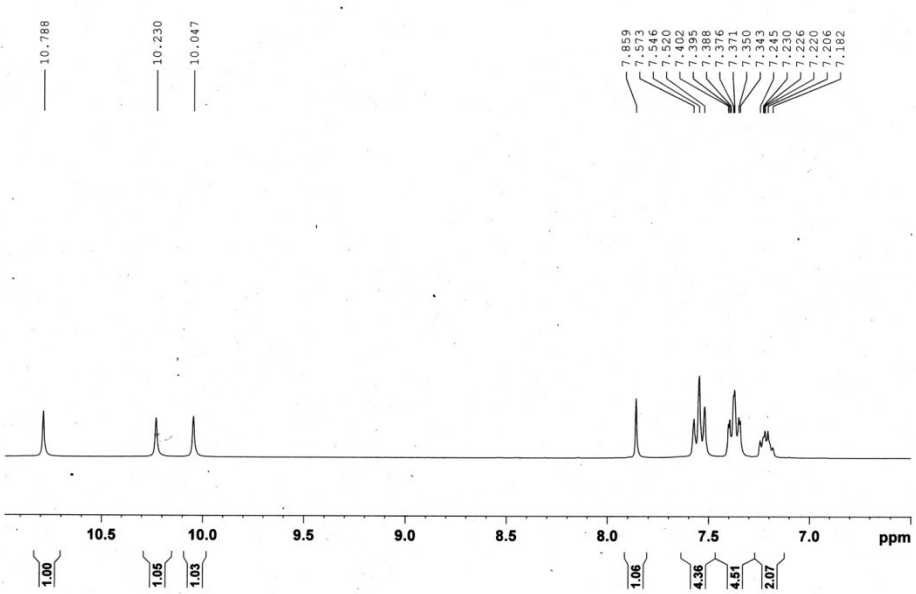

3. Figure S3: Extended NMR spectra of H_2L^1

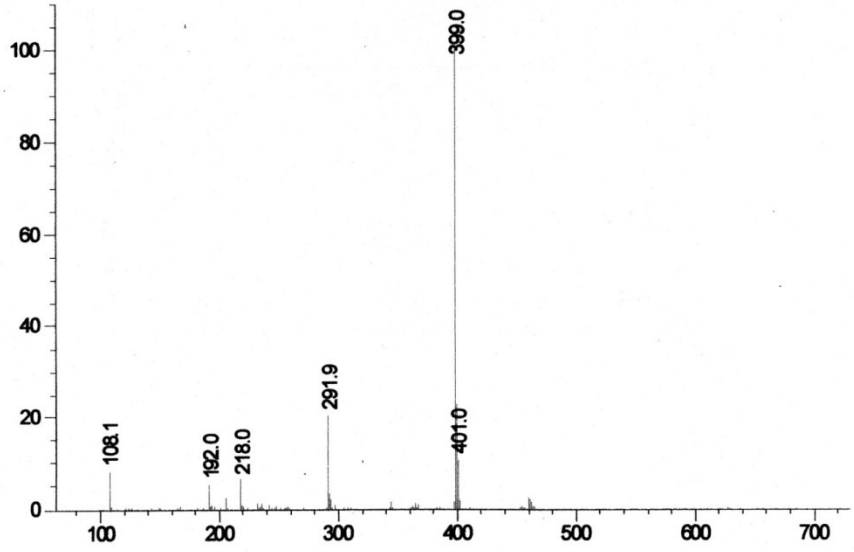

4. Figure S4: Mass spectra of H_2L^2

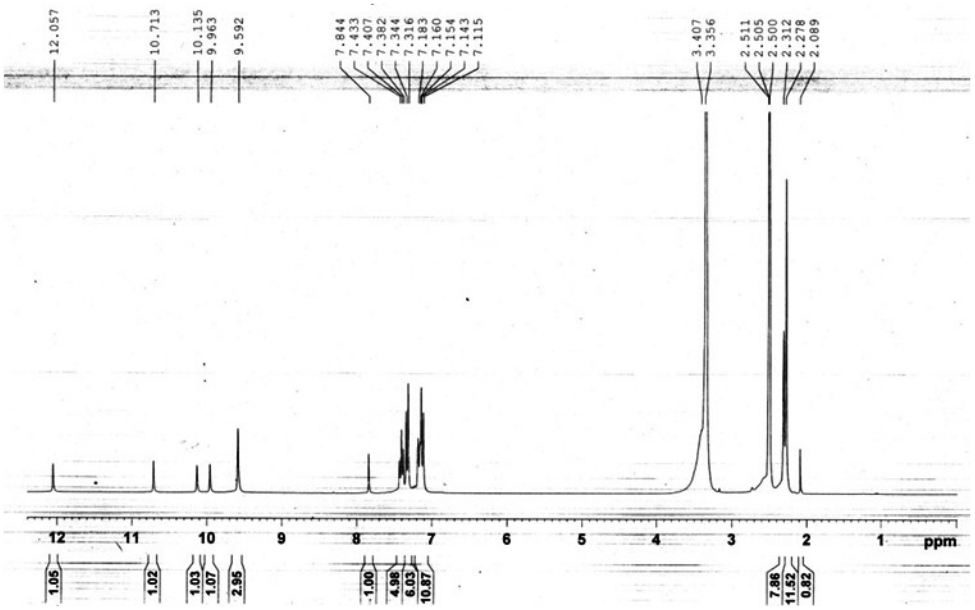

5. Figure S5: NMR spectra of H_2L^2

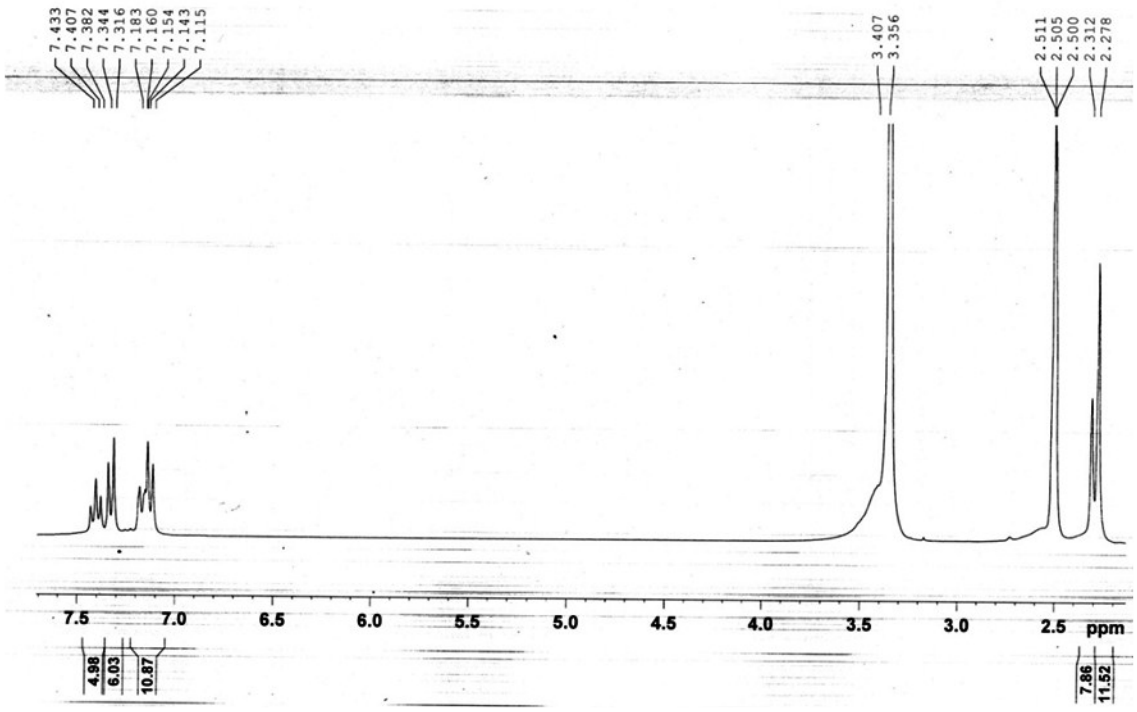

6. Figure S6: Extended NMR spectra of H_2L^2

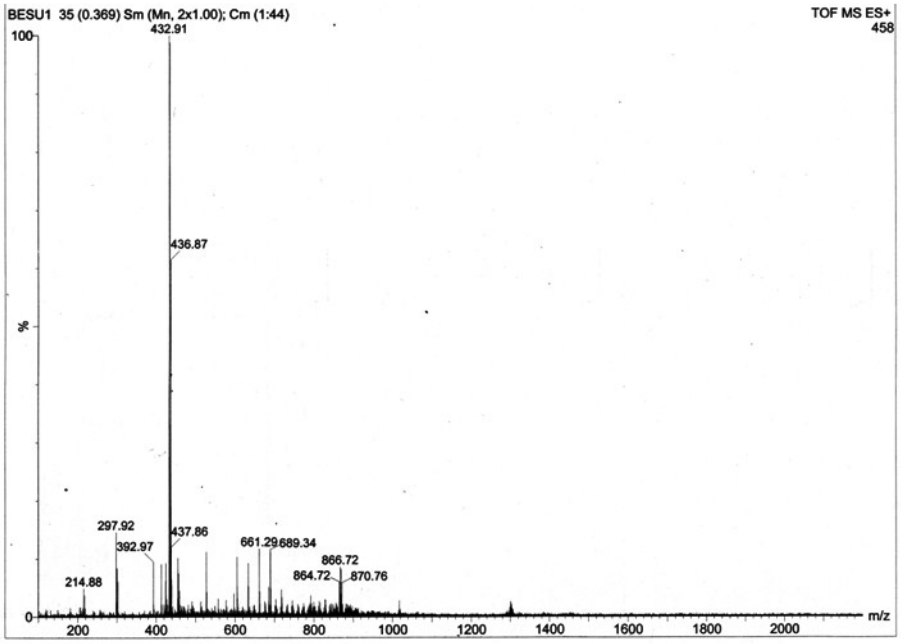

7. Figure S7: Mass spectra of complex **1**

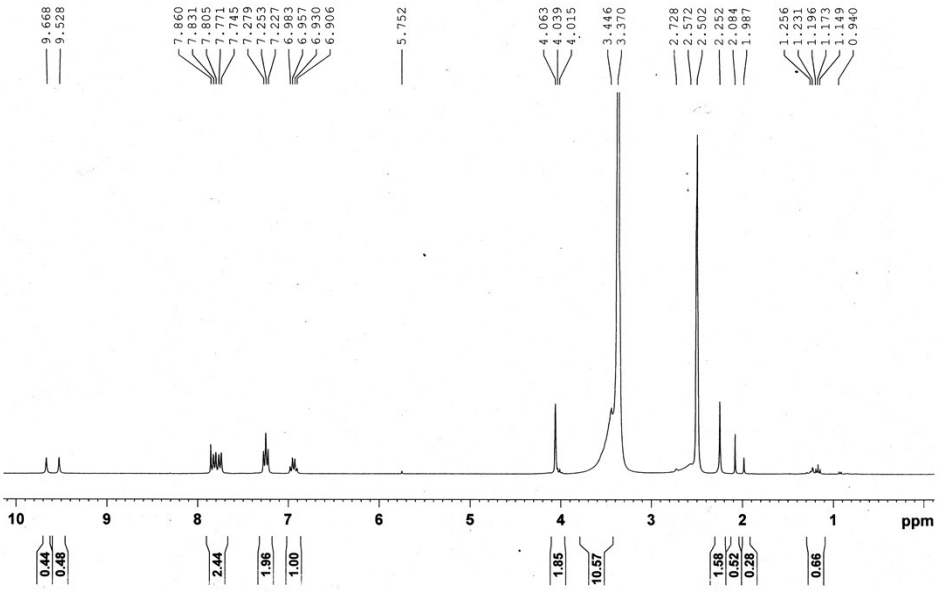

8. Figure S8: NMRspectra of complex **1**

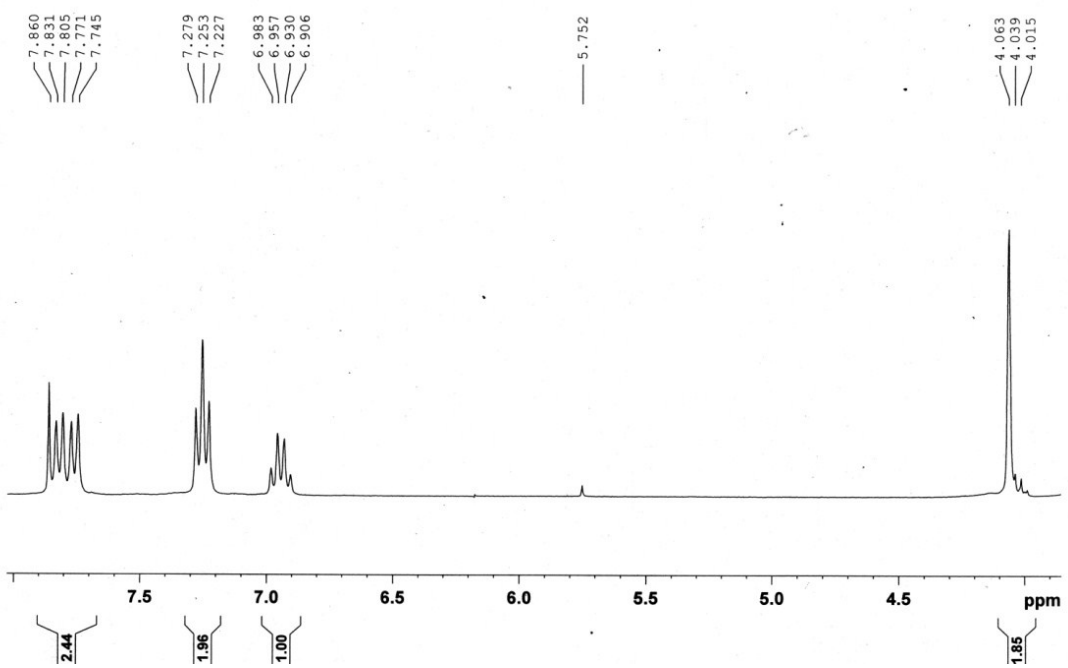

9. Figure S9: Extended NMR spectra of complex **1**

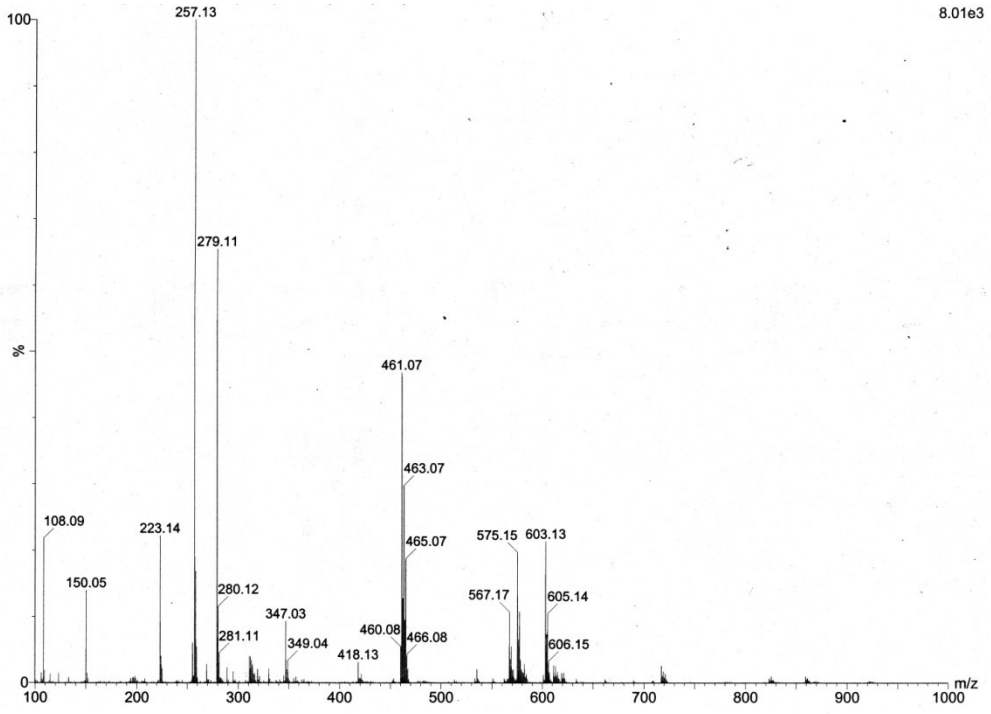

10. Figure S10: Mass spectra of complex **2**

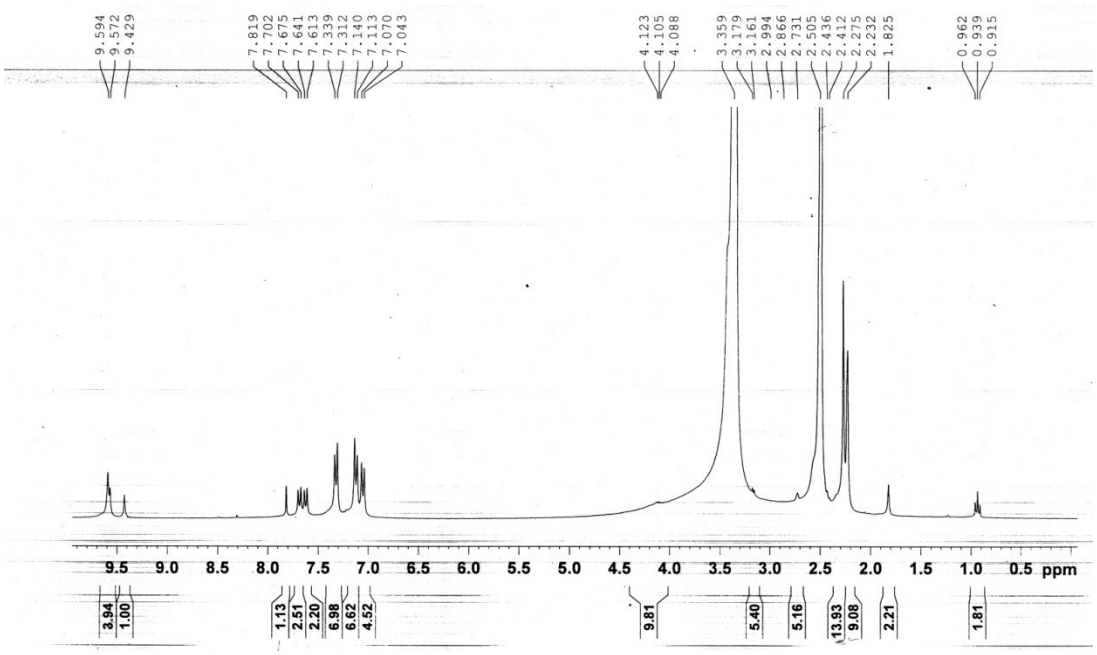

11. Figure S11: NMR spectra of complex **2**

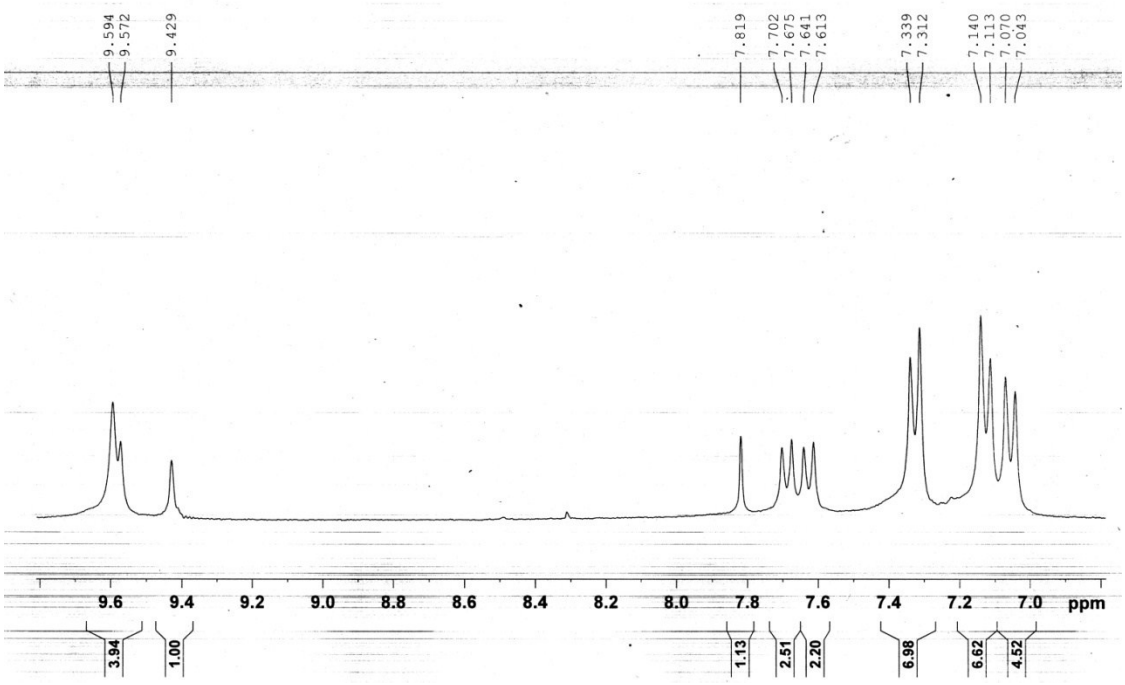

12. Figure S12: Extended NMR spectra of complex **2**

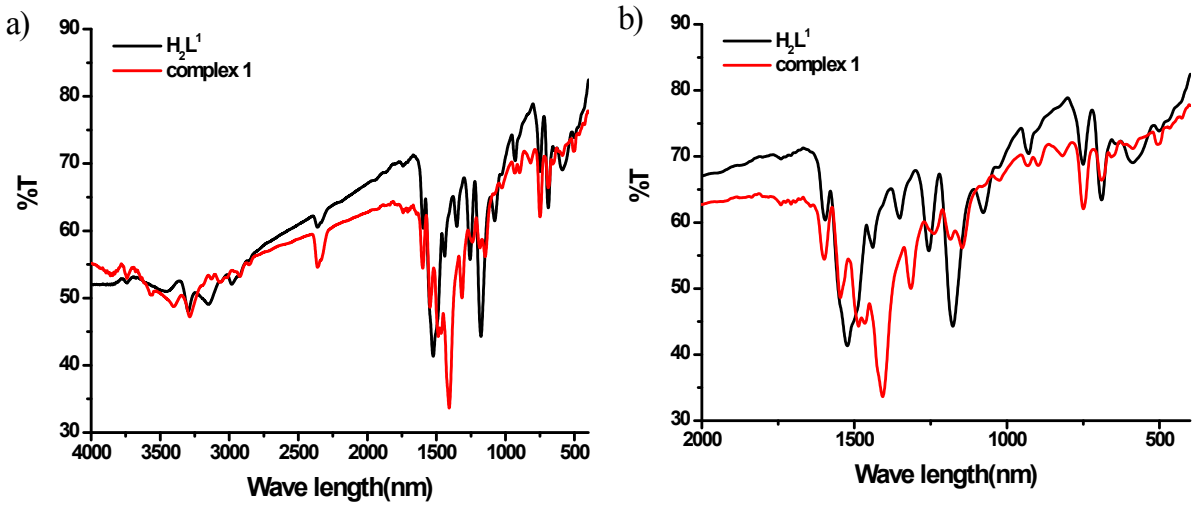

13. Figure S13: IR spectra of L^1 H_2 and complex **1**

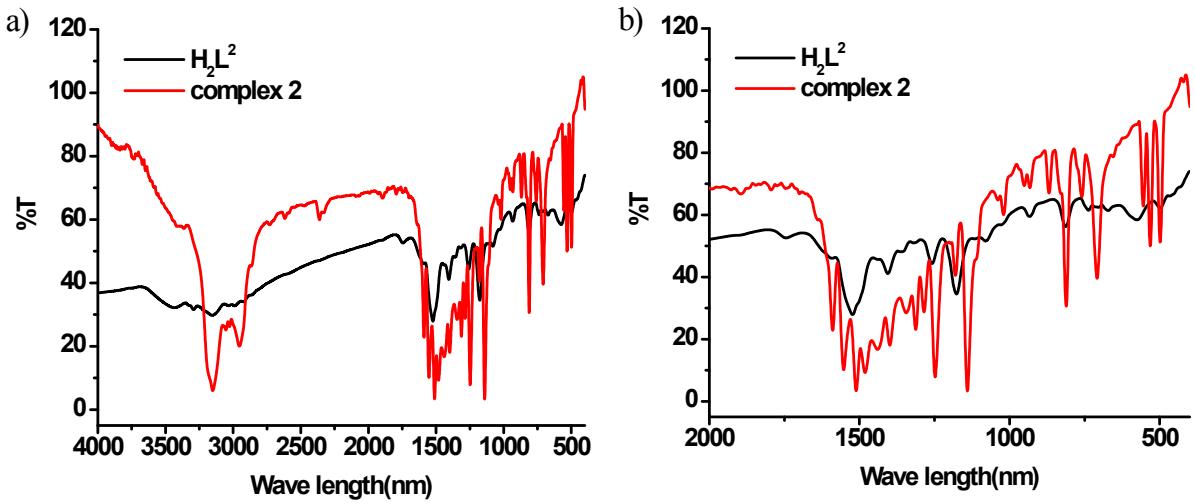

14. Figure S14: IR spectra of L^2 H_2 and complex **2**

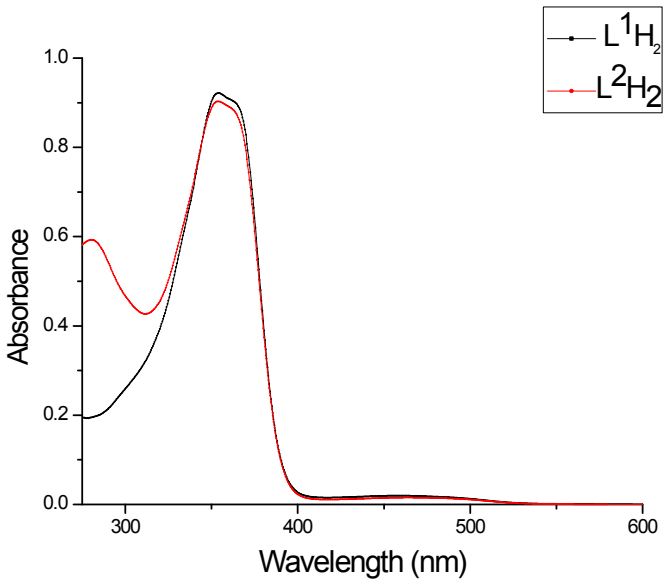

Electronic spectra of the free ligands in DMF solution.

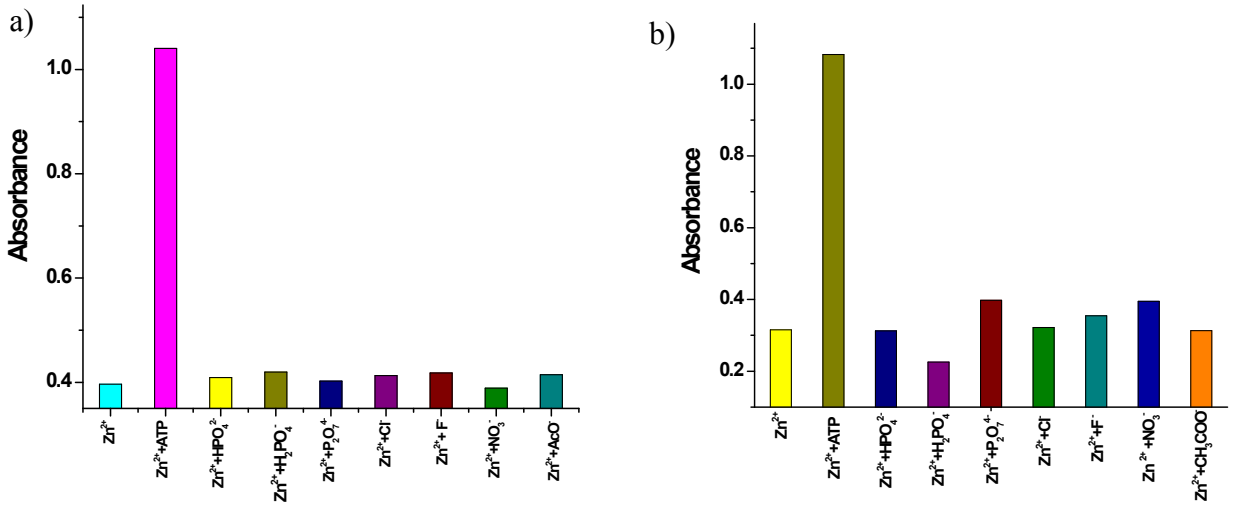

15. Figure S15:UV-vis absorption change of complexes **1** and **2** (1 x 10^{-5} M) in the presence of 24 equiv of different anions at a) Complex **1** at 343 nm and b) complex **2** at 260 nm.

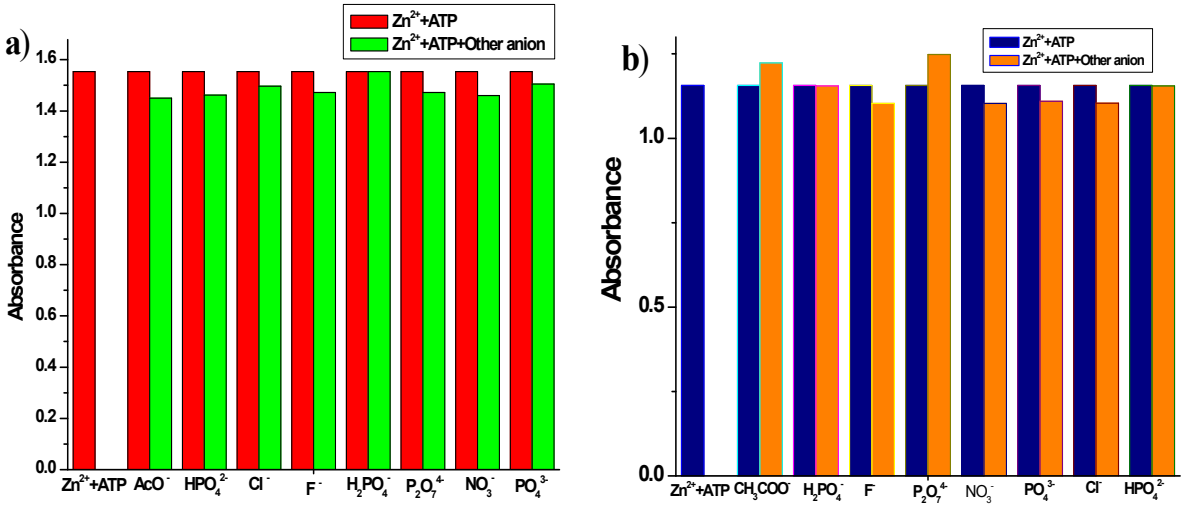

16. Figure S16: a) Red bars: UV-visible absorbance of complex **1** (1 x 10^{-5}) in presence of 8 equiv of ATP. Green bars: UV-visible spectrum of complex **1** (1 x 10^{-5}) in presence of 8 equiv of ATP & 24 equiv of other anions. b) Blue bars: UV-visible absorbance of complex **2** (1 x 10^{-5}) in presence of 8 equiv of ATP. Orange bars: UV-visible spectrum of complex **2** (1 x 10^{-5}) in presence of 8 equiv of ATP & 24 equiv of other anions

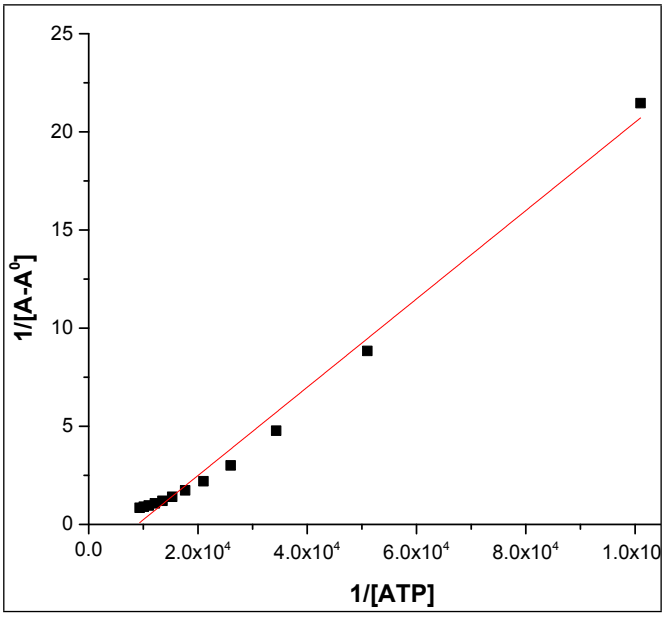

(a)

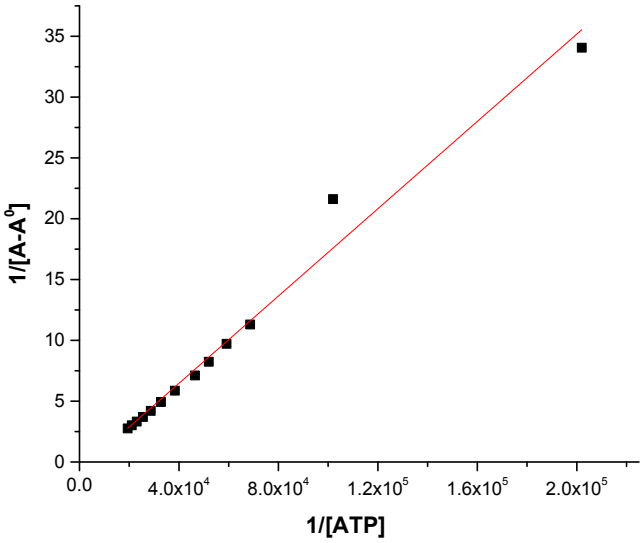

(b)

17. Figure S17: Benesi-Hildeband plot for determination of Ka values of complexes **1**(a) and **2**(b) with ATP.

The Benesi-Hildeband equation used is : $1/\Delta A = 1/\Delta A_{max} + (1/K_b[C])\ (1/\Delta Amax)$, where ΔA and ΔA_{max} are the change in absorbance at a given concentration of ATP, and when all the metal complex is fully bound to ATP respectively, [C] = [ATP].

The detection limit DL of **Complexes** for ATP was determined from the following equation: DL = K× Sb1/S. Where K = 2 or 3 (we take 2 in this case); Sb1 is the standard deviation; S is the slope of the calibration curve.

a)

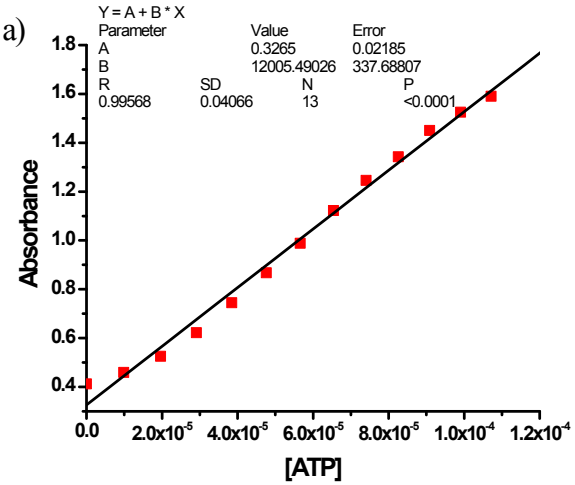

b)

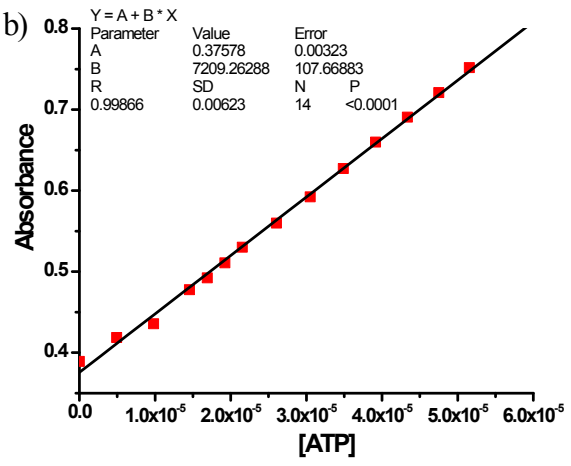

18. Figure S18: Detection limit and calibration curves of a) complex **1** and b) complex **2** with ATP.

From the Absorbance vs. [ATP] graphs (S17), we get slope = 12005.49026, and Sb1 value is 0.04066 for complex **1**. Thus using the formula, we get the Detection Limit for Complex **1**= 6.7×10^{-6}. Similarly for complex **2** Detection Limit = 1.7×10^{-6}.

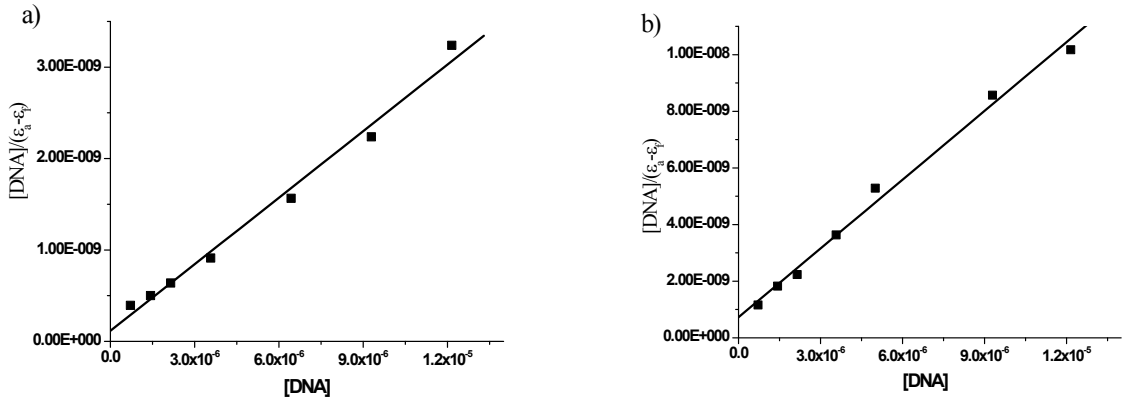

19. Figure S19: Plots of $[DNA]/(\varepsilon_a - \varepsilon_f)$ vs. [DNA] for the titration of DNA with the a) complex **1** b)complex **2**.

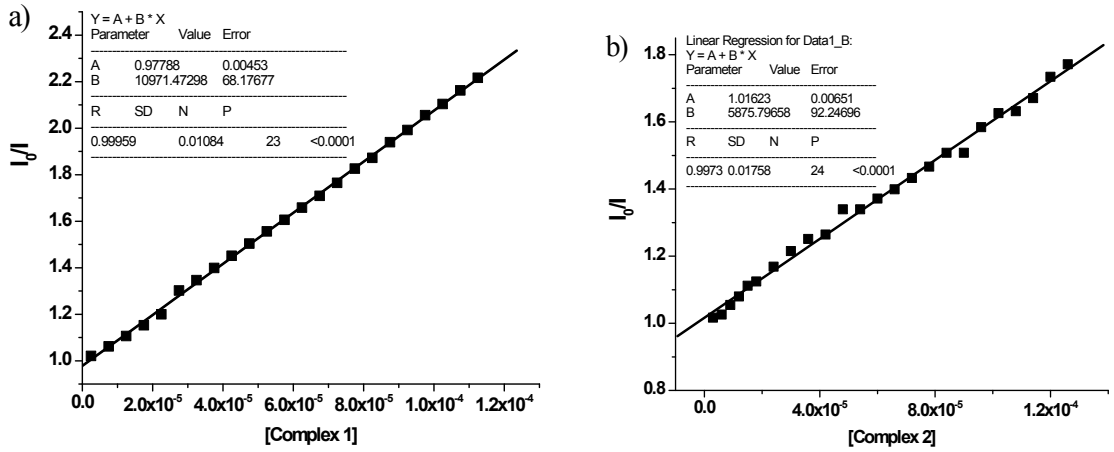

20. Figure S20: Plot of a) I_0/I vs. [Complex **1**] b) I_0/I vs. [Complex **2**].

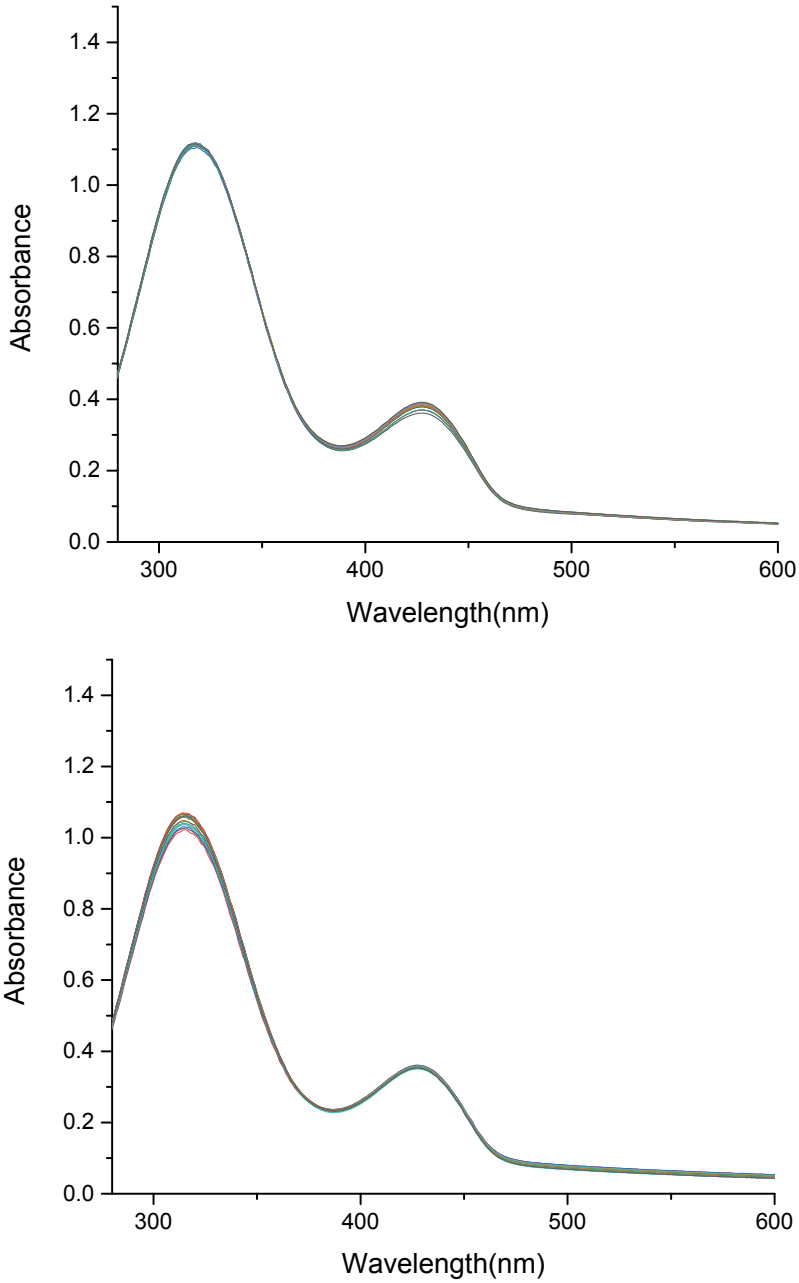

21. Figure S21. Time dependent spectra of PNPP (10^{-4} M) and PNPP(10^{-4} M) in presence of $Zn(OAc)_2$ solution (10^{-5} M).